ELSEVIER

Journal of Wind Engineering
and Industrial Aerodynamics 67 & 68 (1997) 425–436

JOURNAL OF
wind engineering
AND
industrial
aerodynamics

Application of k–ε model to the stable ABL: Pollution in complex terrain

Asmund Huser*, Pål Jahre Nilsen, Helge Skåtun

Det Norske Veritas, Veritasveien 1, N-1322 Høvik, Norway

Abstract

A procedure for the prediction of stable atmospheric boundary layers (ABL) over complex terrain is developed. The standard k–ε model and the computer programme CFX are used as a basis. The turbulence model is modified for the prediction of stable ABL according to recent published works. The procedure employs databases containing topology, road and traffic data, and is applied to estimate ground pollution concentrations in a stable atmosphere over rough terrain. Examples from road planning in Drammen City show comparison with measurements and effects of planned roads.

Keywords: Air pollution; Environmental aerodynamics; Boundary layers; Computational fluid dynamics

1. Introduction

The aim of this work is to increase knowledge and abilities for prediction of pollution dispersion in a stable atmosphere and over complex terrain. The use of advanced tools, such as 'Computational Fluid Dynamics' (CFD) codes and topography and pollution databases, is essential in this work. The location of Norway, being at a high latitude, causes reduced sun radiation and hence long periods with stable air, especially in the winter. Together with increasing traffic this causes air pollution to become a serious problem, and thus the need for a tool for prediction of pollution dispersion to be developed [1,2].

The two-equation k–ε model is the most popular first order turbulence model. Several variations of this model exist (e.g. k–l model, k–ω model); they have in common that the two turbulence equations produce an *isotropic* eddy-viscosity parameter which is applied to both the momentum equations and the pollution transport equation. The implication of an isotropic eddy-viscosity is that a pollutant

* Corresponding author. E-mail: ahu@dnv.com.

PII S0167-6105(97)00091-3

will dilute equally fast in all three directions. The buoyancy extended k–ε model applied here is due to Rodi [3]. The work of Duynkerke [4] shows that the isotropic k–ε model compares well with measurements when simulations are performed on a flat atmospheric boundary layer. The two equation q^2–l model of Ref. [5] is also found to predict well the flow over a nearly 2D hill. Based on this, the first order isotropic models perform well for relatively simple geometries, stable atmospheres, and relatively smooth surfaces. The present work applies this turbulence model to a real case on rough terrain and with topology, and reports its performance.

2. Prediction method for the stable ABL

The Reynolds averaged Navier–Stokes equations are solved by the standard programme CFX-F3D (formerly FLOW3D from Harwell). Flow calculations are performed by specifying the wind, temperature and turbulence quantities on the inlet planes, and calculating the air flow and heat transfer in the computational domain until steady state conditions are reached. A quasi steady state is obtained with a constant cooling rate at the surface. This implies that the temperature will decrease downwind, but turbulence quantities and wind are constant. Effluents are released as a source to a transport equation for passive scalar (NO_x). This equation is solved using the constant steady state velocity and temperature field obtained in the flow calculations. The assumption of steady flow conditions is justified by a slow development in the atmospheric conditions under the situations considered. The situations considered are typically a winter day with a stable atmosphere created by low sun radiation with no convective wind generation.

Further assumptions to the flow equations are that no Coriolis force is included, and that the buoyancy term in the vertical momentum equation is neglected. The Coriolis force causes the velocity to turn with height. In the present calculations, the wind is directed by the direction of the valley, and hence the geometry effects are assumed to dominate the Coriolis effect. The buoyancy term in the vertical momentum equation is neglected because it requires special treatment of the pressure outflow boundary conditions. Neglecting the buoyancy effect in the vertical momentum equation causes no wind to occur due to vertical density gradients. These effects may be significant when heavy cold or humid air is draining out from a higher altitude location. In the present model, to compensate for this, drainage flows are forced on the solution when these are known to occur. This is done by specifying a drainage flow as an inlet to the domain at the actual location. The present method is therefore not able to determine where drainage flows will occur. This must be known from observations and field measurements. However, with a mode detailed model, this effect may be incorporated.

2.1. Turbulence model

The k–ε turbulence model is applied in the calculations. The constants used are listed in Table 1. The constants $C_{\varepsilon 1}$ and $C_{\varepsilon 2}$ are standard values from Ref. [6]. Ref. [4]

Table 1
Constants used in the k-ε model

$C_{\varepsilon 1}$	$C_{\varepsilon 2}$	$C_{\varepsilon 3}$	C_{μ}
1.44	1.92 (and 1.83)	1	0.033

uses $C_{\varepsilon 2} = 1.83$ for an atmospheric flow calculation. A reduction of $C_{\varepsilon 2}$ causes the destruction of ε to be reduced, hence ε itself will increase. In the present flat terrain model, the value $C_{\varepsilon 2} = 1.83$ is also used to indicate the effect of this parameter. In the current buoyancy extended version of the code [3], production of ε by buoyancy is zero for stable conditions. Production of k by buoyancy is also zero according to Ref. [3]. The eddy-viscosity is given by

$$\nu_{\mathrm{T}} = C_{\mu}\frac{k^2}{\varepsilon}, \tag{2.1}$$

where k is the turbulent kinetic energy, and ε is the dissipation rate of turbulent kinetic energy. The value of C_{μ} is smaller than the standard value found by wind tunnel tests which is 0.09. In an atmospheric boundary layer C_{μ} is smaller than in a wind tunnel test because production of turbulence is not only due to wall shear stress, but also gravity waves, topography and other large-scale effects.

2.2. *Inlet conditions*

Inflow profiles are given for the wind speed (u), potential temperature (θ), turbulent kinetic energy (k) and dissipation rate of turbulent kinetic energy (ε). By enforcing these profiles on the inlet planes, the wind speed and the atmospheric stability are defined. The surface roughness, stability class and the surface heat transfer rate are parameters that are set to specify the state of the atmosphere. These parameters are both set on the surface and on the inlet profiles. Formulas for the inflow profiles are given in Ref. [7] and read:

$$u = u_{*}\frac{1}{\kappa}[\ln(z/z_0) - \psi_{\mathrm{M}}(z/L) + \psi_{\mathrm{M}}(z_0/L)], \tag{2.2}$$

where $\psi_{\mathrm{M}} = -17(1 - \mathrm{e}^{-0.29z/L})$, and $\kappa = 0.41$ is the von Karman constant;

$$\Delta\theta = \theta_{*}\frac{1}{\kappa}[\ln(z/z_2) - \psi_{\mathrm{H}}(z/L) + \psi_{\mathrm{H}}(z_2/L)], \tag{2.3}$$

where $\psi_{\mathrm{H}} = -5z/L$ and z_0 is used as a reference length of temperature. The difference between the surface temperature and the air temperature at z is given by $\Delta T = \Delta\theta - gz/C_p$. The surface roughness z_0 may vary from 0.0002 m for open sea to 1 m for suburbs and forests [8]. In the present cases, a constant value of 1 m is used at

Table 2
Mean Obukov length for stable atmospheres, Ref. [7]

Class parameter	*d*	*e*	*f*	*g*
Mean Obukov length, *L* (m)	10000	350	130	60

the inlet and at the surface. The friction velocity (u_*) is found by inserting a known reference wind speed into Eq. (2.2). The reference wind speed at 10 m above the surface is applied. The temperature scale (θ_*) is found by the definition of the Obukov length scale:

$$L = \frac{u_*^2}{\kappa g \theta_* / T}. \tag{2.4}$$

The Obukov length is a measure of stability and defines the stability classes in Table 2, where *d* is neutral and *g* is very stable.

Another important parameter is the boundary layer depth, *h*, which is the height where the velocity shear vanishes. It is given in Ref. [4]:

$$h = 0.4\sqrt{u_* L/f}, \tag{2.5}$$

where *f* is the Coriolis parameter. ($f = 0.000125$/s in Drammen.) The heat flux at the ground is given by $H = \theta_* u_* \rho C_p$ (W/m^2). In a stable boundary layer the effects caused by velocity shear and density stratification have opposite effects on dilution. The shear layer produces turbulence and hence enhances mixing, whereas the stable air reduces mixing. The correct combinations of the stability parameters (Obukov length) and velocity shear (roughness height) may be estimated when comparing measurements and model predictions.

The inlet profiles for the turbulence parameters k and ε are found in Ref. [4] and read:

$$k = \frac{u_*^2}{\sqrt{C_\mu}}\left(1 - \frac{z}{h}\right)^2, \tag{2.6}$$

$$\varepsilon = \frac{u_*^3}{\kappa}\left(\frac{1}{z} + \frac{4}{L}\right). \tag{2.7}$$

Combining Eqs. (2.1), (2.6) and (2.7), the normalised eddy-viscosity at the inlet is

$$\frac{\nu_T}{\kappa u^* h} = \frac{(1 - z/h)^4}{h/z + 4h/L}. \tag{2.8}$$

2.3. Wall boundary conditions

Wall boundary conditions for the velocity, temperature and scalar are given by the law of the wall which reads for a general variable ϕ:

$$\frac{\phi}{\phi^*} = \frac{\sigma_\phi}{\kappa} \ln\left(\frac{z}{z_0}\right), \tag{2.9}$$

where σ_ϕ is the turbulent Prandtl number (= 0.9 for temperature and scalar).

2.4. Outlet, sides and upper boundary

Outlet boundary conditions are given by specifying the pressure, and setting no gradients in the flow direction on the other variables. On the side planes of the domain and the upper boundary, symmetry conditions are imposed. That is to say no air is entering or leaving these boundaries.

2.5. Equation of state

The equation of state applies the weakly compressible assumption:

$$\rho = \frac{p_{\text{ref}} w}{R\theta}, \tag{2.10}$$

where $p_{\text{ref}} = 1.013105$ Pa is constant, $w = 29$ is the molecular weight of air and $R = 8314$ J/(K kmol) is the universal gas constant. The potential temperature (θ) is used in the calculations in order to compensate for the weakly compressible assumption.

2.6. Estimation of sources

The major NO_x sources used for this study are emissions from vehicles. In addition emissions from a few major industry stack sources are included, as well as diffuse sources, mainly originating from domestic heating.

The emissions from vehicles are implemented as quasi-line-sources. The road network is divided into line segments. For each segment the release per road length and time unit are computed, based on parameters such as the amount of vehicles, average speed, fraction of heavy trucks and the slope of the road. Minor roads, having less than 5000 vehicles passing per day are excluded.

Each linear road segment contributes to the source of the cells corresponding to the length of the segment within each cell. When the contributions to each horizontal grid cell are added for all line segments, the total source for each cell is applied as a point source in the grid cell closest to the ground. Emissions from vehicles contribute to approximately 80% of the total sources.

Diffuse sources are also added as a point source in the grid cell closest to the ground. For stack sources, standard plumerise formulas are applied to find the equilibrium height of the plume, and the stack sources are entered into the model in the grid cell corresponding to the position of the stack and a height above the ground which equals the equilibrium height.

3. Results and discussion

Results from two simulation models are presented here. First, flow over a flat terrain and second, flow over topology. For both models the development of the boundary layer is presented in terms of eddy-viscosity profiles. The eddy-viscosity is defined in Eq. (2.1) and is important for pollution dilution because it enters the diffusion term in the passive scalar equation.

3.1. Flow over flat terrain

A simple geometrical model measuring 10 by 5000 m is used. Velocity, temperature and turbulence profiles, given in Section 2.2, are set on the inlet. The parameters for the two cases presented here are given in Table 3. The normalised eddy-viscosity profiles are presented in Fig. 1 indicating that the eddy-viscosity increases when going downwind. The measured maximum value of normalised eddy-viscosity [4] is 0.04, indicating that the present calculations are over-predicting the eddy-viscosity. Measurements that make the basis for the normalised eddy-viscosity in Ref. [4] are from flat terrain with little topology and low roughness $z_0 = 0.01$ m. In the high roughness case, a roughness of $z_0 = 1$ m is used. The over-prediction of normalised eddy-viscosity is smaller for smooth terrain than for rough terrain. Measurements of eddy-viscosity in rough terrain are lacking, and hence the correct value of the maximum eddy-viscosity is unknown. Reducing the $C_{\varepsilon 2}$ parameter from 0.92 to 0.83 causes the maximum eddy-viscosity to decrease toward the measured value (see

Table 3
Parameters used in flow over flat terrain and topology

	Case 1, Rough surface	Case 2, Smooth surface	Run 3, Topology model
Wind speed at 10 m (m/s)	1.5	4	1
Stability class	e	f	f
Roughness z_0 (m)	1	0.01	1
u^* (m/s)	0.26	0.23	0.16
θ^* (K)	0.013	0.029	0.014
h (m)	340	196	163
L (m)	350	130	130
Ground heat flux (W/m^2)	− 3.87	− 13.4	− 2.4

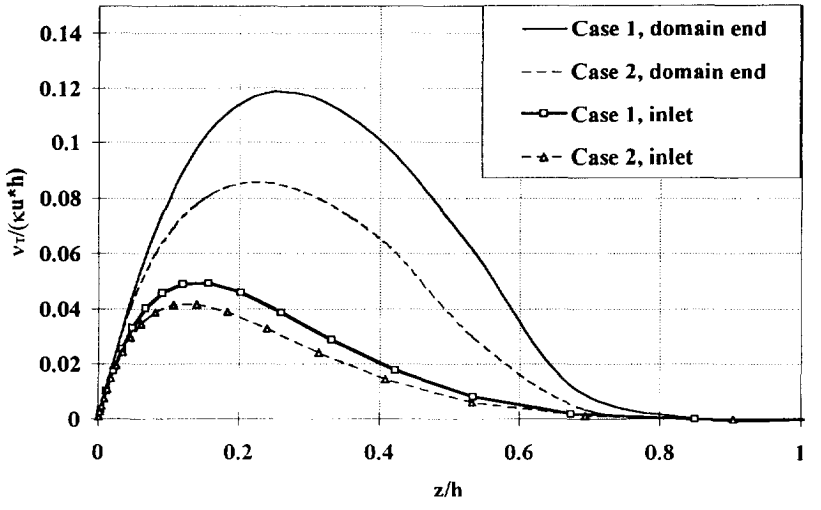

Fig. 1. Normalised eddy-viscosity at the inlet and 5 km downwind the inlet. The inlet profiles are given by Eq. (2.8) and compared with measurements for smooth surfaces. Comparing smooth and rough surface model. $C_2 = 0.92$.

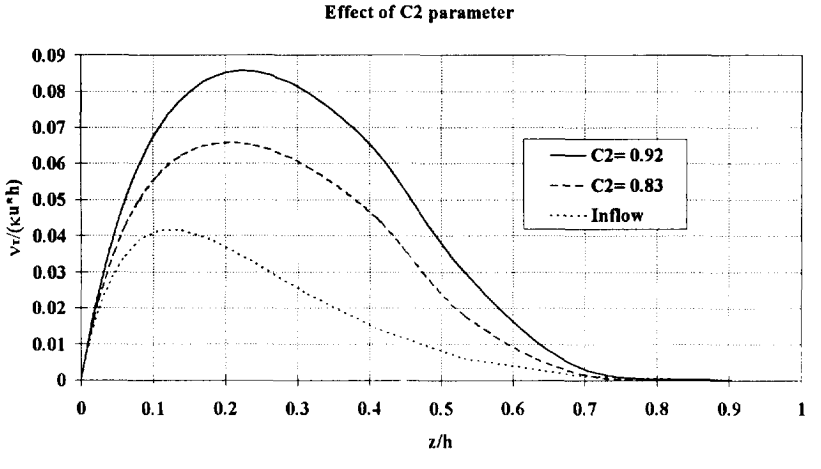

Fig. 2. Flow over smooth flat terrain, case 2. Eddy-viscosity profiles 5 km downwind inlet. The inlet profile is given by Eq. (2.8) and compared with measurements for smooth surfaces.

Fig. 2). This indicates that the value of 0.83 is more appropriate for atmospheric flows. Still, the value of 0.83 does not give the correct behaviour, indicating the uncertainty of this parameter. The grid resolution has a small impact on the solution in the outer part of the boundary layer as indicated in Fig. 3.

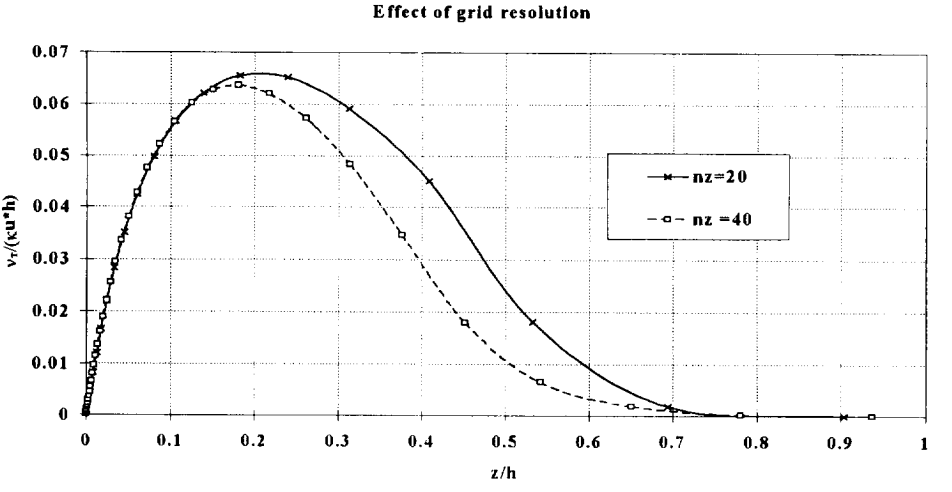

Fig. 3. Flow over smooth flat terrain, case 2. Eddy-viscosity profiles 5 km downwind inlet. $C_2 = 0.83$. Grid resolution: $n_x = 20$ and $n_z = 20$ (crosses); and $n_x = 50$ and $n_z = 40$ (squares), where n_x and n_z are the number of nodes horizontally and vertically, respectively.

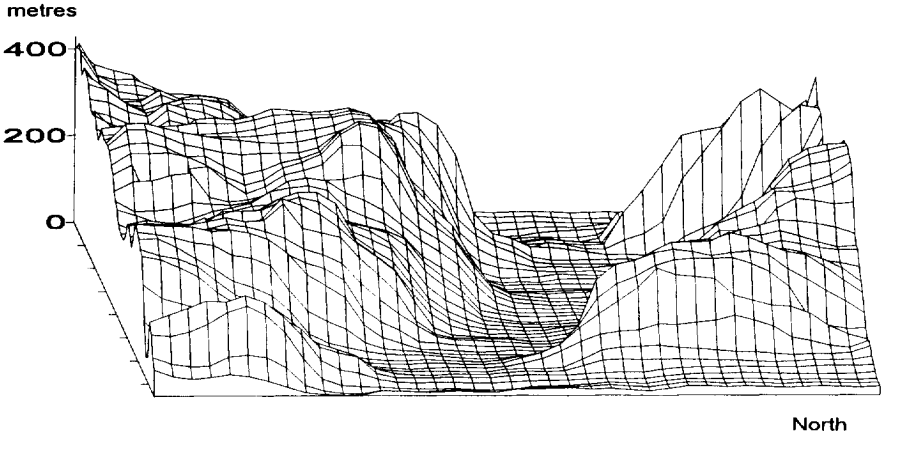

Fig. 4. Model of the Drammen Valley. The north–south distance is 16 km, and the east–west distance is 20 km.

3.2. *Flow over topology*

The city model contains an area of 20 by 16 km including the Drammen valley and the surrounding hills, which are up to 400 m high (see Fig. 4). In this model, the finest grid cells are down to 100 by 100 m.

Results show the normalised eddy-viscosity for one of the runs. The parameters are presented in Table 3. The normalised eddy-viscosity is shown to increase above the

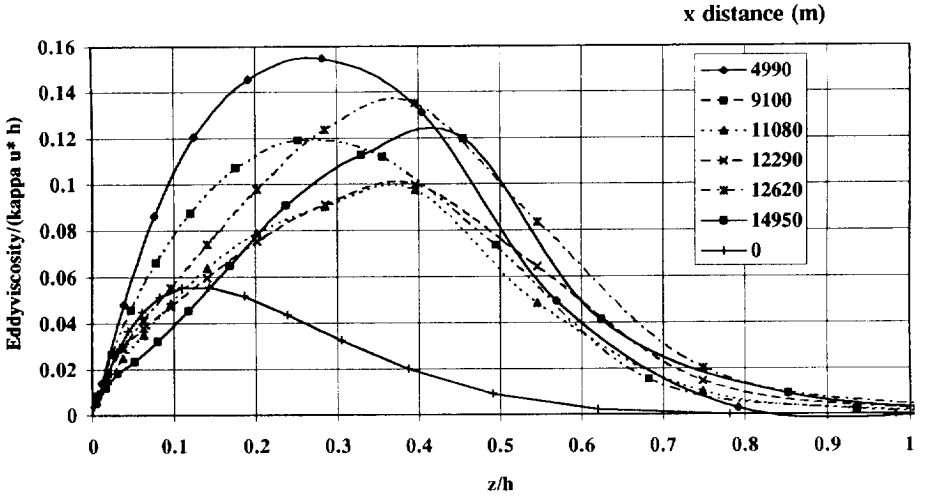

Fig. 5. Normalised eddy-viscosity at six locations downwind the inlet. The inlet profile is given by Eq. (2.8) and compared with measurements for smooth surfaces.

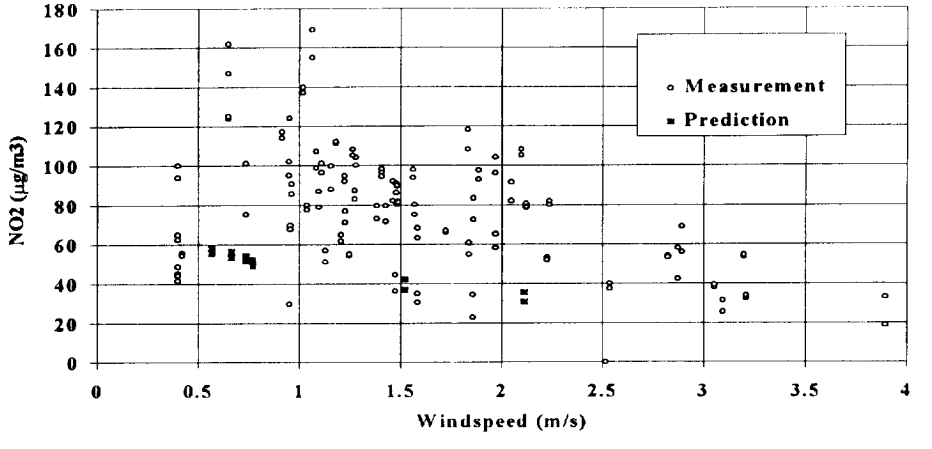

Fig. 6. Comparison of predicted concentration of NO_2 with measured values.

inlet value of 0.055 (see Fig. 5). After 5000 m the maximal value of the normalised eddy-viscosity stays below 0.14 indicating that the boundary layer is not developing further. A surface roughness of 1 m is above the roughness of 0.01 which is used in Ref. [4], explaining some of the discrepancies.

3.3. *Evaluation of the model*

The model was found to give the right trend of pollution concentration with increasing wind speed (see Fig. 6). Both the surface roughness and the stability

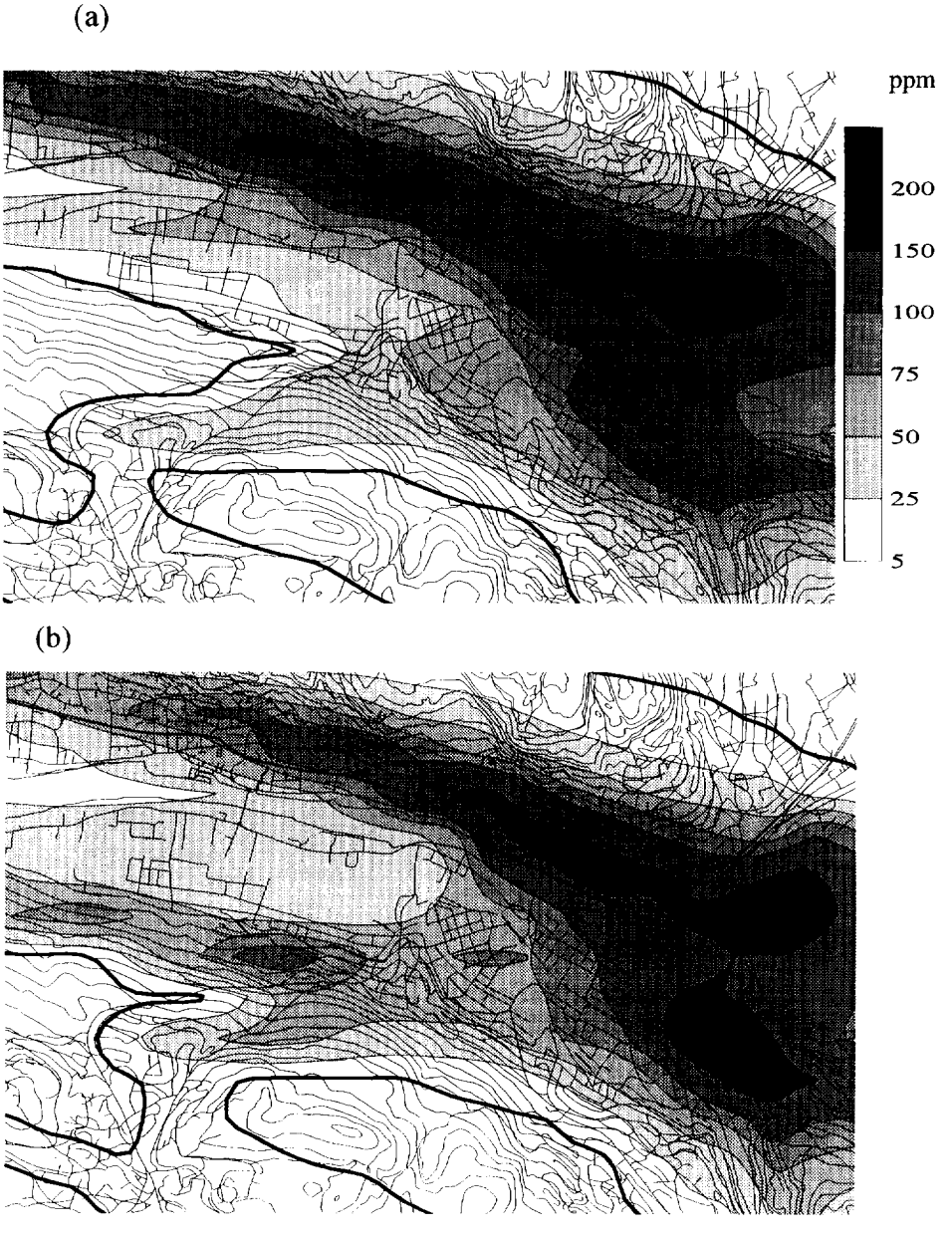

Fig. 7. Comparison of NO_x concentration in the Drammen Centre for existing roads (a) and planned roads in 2005 (b).

parameters were fixed, based on qualitative judgements, prior to the calculations. The present results indicate that too high roughness and too weak stability has been used, both factors causing too much mixing and hence lower concentrations than measured on the worst days in Drammen. By specifying the stability and surface roughness parameters, the corresponding atmospheric conditions may be simulated. The present results may be used as a basis for selecting other values for the roughness and stability parameters.

The model is found useful for predicting airpollution in e.g. road planning or planning of location of other releases to the atmosphere. As an example, Fig. 7 shows the effect of planned roads in Drammen on NO_x concentration.

Results show that the *normalised* eddy-viscosity is over-predicted compared to measured values [4]. This may be caused by three factors: Too high surface roughness, adjustments to the $C_{\varepsilon 2}$ parameter and the isotropic model.

The surface roughness length of forests and suburbs (1 m) is used in the whole domain in the Drammen model. Measurements of the eddy-viscosity (or other turbulence parameters) found in the literature are uncertain for such high roughness, therefore the value of the calculated eddy-viscosity cannot be directly verified. Also, the surface roughness does vary in the Drammen area from $z_0 = 0.01$ m over flat areas and water surfaces to the order of 1 m over forests and urban areas. A lower surface roughness may therefore be justified. In a more detailed model, a variable surface roughness should be given over the area.

The turbulence constant $C_{\varepsilon 2}$ takes different values in the literature, and could be adjusted further to calibrate the model against measured pollutant concentrations.

Atmospheric stability is specified on the flow inlets by the temperature profile, and on the surface by the heat flux from the air. A logarithmic temperature profile is used, which has the steepest temperature gradient near the surface. A more detailed model will have to include the possibility to model inversion layers and anisotropy turbulence models. An inversion layer acts as a 'lid' on the valley and will trap the pollutants inside. The logarithmic temperature profile is an assumption which is difficult to check because no profile measurements have been performed in Drammen. Observations of temperature profiles elsewhere [7] show both profiles with the strongest gradient at the ground and profiles with a gradient both at the ground and in a layer above the ground. Implementation of an anisotropic turbulence model will cause the vertical dilution to reduce. This will enable us to predict more correctly the inversion which is trapping the pollutant inside the valley.

The grid resolution may also be a small source of inaccuracies. It is important to concentrate the grid-lines where the gradients are highest. Therefore, when reducing the surface roughness, the grid-lines in the z direction must be refined near the ground.

Acknowledgements

This study has been sponsored by Statens Vegvesen Buskerud (the Road Authorities of Drammen). The support of the contact person, Mr. Bjørn Haram, is much

appreciated. The authors would also like to acknowledge the valuable comments of Dr. Ivar Nestaas and Mr. Sigmund Olavsen. Funding provided by Det Norske Veritas is appreciated.

References

[1] S. Olafsen, Forstudie luftmodell – Drammen og Nedre Eiker, DNV Industry rapport no. 94-3634, 1994.
[2] A. Huser, P.J. Nilsen, H. Skåtun, Beregning av luftforurensing i Drammen og omegn – Utvikling av beregningsmodell, DNV Industry rapport no. 95-3287, 1995.
[3] W. Rodi, Calculation of stably stratified shear layer flows with a buoyancy – extended K–ε turbulence model, in: J.C.R. Hunt (Ed.), Turbulence and Diffusion in Stable Environments, Oxford University press, Oxford, 1985, pp. 111–143.
[4] P.G. Duynkerke, Application of the E–ε turbulence closure model to the neutral and stable atmospheric boundary layer, J. Atmos. Sci. 45 (5) (1988).
[5] T. Yamada, Simulation of nocturnal drainage flows by a q^2l turbulence closure model, J. Atmos. Sci. 40 (1983) 91.
[6] CFDS-FLOW3D Release 3.3, Users manual.
[7] A.P. van Ulden, A.A.M. Holtslag, Estimation of atmospheric boundary layer parameters for diffusion applications, J. Clim. Appl. Met. 24 (1985).
[8] J. Counihan, Adiabatic atmospheric boundary layers: A review and analysis of data from the period 1880–1972, Atmospheric Environment 9 (1975) 871–905.